

# Susceptibility of rabbits to SARS-CoV-2

**Authors:** Anna Z. Mykytyn, Mart M. Lamers, Nisreen M.A. Okba, Tim I. Breugem, Debby Schipper, Petra B. van den Doel, Peter van Run, Geert van Amerongen, Leon de Waal, Marion P.G. Koopmans, Koert J. Stittelaar, Judith M.A. van den Brand, Bart L. Haagmans

## **Affiliations:**

Erasmus Medical Center, Rotterdam, the Netherlands (A.Z. Mykytyn, M.M. Lamers, N.M.A. Okba, T.I. Breugem, D. Schipper, P.B. van den Doel, P. van Run, M.P.G. Koopmans, B.L. Haagmans)

Utrecht University, Utrecht, the Netherlands (J.M.A. van den Brand)

Viroclinics Biosciences B.V., Viroclinics Xplore, Schaijk, the Netherlands (G. van Amerongen, L. de Waal, K.J. Stittelaar).

**Address for correspondence:** Bart Haagmans, Viroscience department, Erasmus Medical Center, Rotterdam; email: [b.haagmans@erasmusmc.nl](mailto:b.haagmans@erasmusmc.nl)

**Keywords:** Rabbit, SARS-CoV-2, COVID-19, coronavirus

20 **Abstract**

21 Transmission of severe acute respiratory coronavirus-2 (SARS-CoV-2) between livestock and  
22 humans is a potential public health concern. We demonstrate the susceptibility of rabbits to  
23 SARS-CoV-2, which excrete infectious virus from the nose and throat upon experimental  
24 inoculation. Therefore, investigations on the presence of SARS-CoV-2 in farmed rabbits should  
25 be considered.

26

27 **Text**

28 Severe acute respiratory syndrome coronavirus 2 (SARS-CoV-2) caused a pandemic only  
29 months after its discovery in December 2019 (1). Slowing down its spread requires a full  
30 understanding of transmission routes, including those from humans to animals and vice versa. In  
31 experimental settings, non-human primates, ferrets, cats, dogs and hamsters have been found to  
32 be susceptible to SARS-CoV-2 infection (2-4). Moreover, ferrets, cats and hamsters were able to  
33 transmit the virus via the air (2, 4, 5). In domestic settings, both dogs and cats have been found to  
34 carry the virus, displaying very mild to more severe symptoms, respectively (5). Recently,  
35 SARS-CoV-2 has been isolated from mink at multiple Dutch farms. Workers at those farms  
36 carried viruses that were highly similar to the viruses detected in mink and phylogenetic analyses  
37 supported transmission from mink to workers (6). Thus, measures to control the spread of SARS-  
38 CoV-2 should also include preventing spill over into potential reservoirs, especially since  
39 infectious agents can spread rapidly in livestock due to the high densities at which some animals  
40 are kept. Given the fact that rabbits are commonly farmed worldwide, we investigated the  
41 susceptibility of rabbits to SARS-CoV-2.

42

43

#### 44 **The study**

45           Angiotensin converting enzyme 2 (ACE2) dictates the host range for SARS  
46 coronaviruses (7), because it engages the viral spike (S) glycoprotein for cell attachment and  
47 fusion of the viral and host membranes (8). Contact residues of human and rabbit ACE2 critical  
48 for binding S are relatively well conserved (9). We overexpressed ACE2 from different species  
49 on a receptor-deficient cell line followed by SARS-CoV-2 pseudovirus or authentic virus  
50 infection. Successful infection of both SARS-CoV-2 pseudovirus and authentic virus was  
51 observed for human, rabbit and the Chinese horseshoe bat (*Rhinolophus sinicus*) ACE2 (Figure  
52 1, panel A and B). The ACE2 from a distantly related bat, the great Himalayan leaf-nosed bat  
53 (*Hipposideros armiger*), did not support infection and served as a negative control. Transfection  
54 of rabbit ACE2 rendered cells susceptible to SARS-CoV-2 infection demonstrated by a clear  
55 overlap between infection and ACE2 expression (Figure 1, panel C).

56           Next, we inoculated three rabbits with  $10^6$  tissue culture infectious dose 50 (TCID<sub>50</sub>)  
57 SARS-CoV-2 for a 21 day follow up. None of the inoculated animals showed clinical signs of  
58 infection. As shown in Figure 2 (panel A), we found viral RNA in the nose for at least twenty-  
59 one days (mean shedding of 15.33 days, SD=5.13), up to fourteen days in the throat (mean  
60 shedding of 11.33 days, SD=2.52) and up to nine days in the rectum (mean shedding of 5 days,  
61 SD=3.61). Infectious virus shedding from the nose lasted up to seven days (mean shedding of  
62 6.67 days, SD=0.58) with a peak at day two, followed by a second peak at day seven post  
63 inoculation (p.i.) (Figure 2, panel B). In the throat, infectious virus was detected only on day one

64 p.i. for one animal. No infectious virus was detected in rectal swabs. All animals followed up to  
65 day 21 seroconverted with plaque reduction neutralization test (PRNT<sub>50</sub>) titers of 1:40, 1:320 and  
66 1:640.

67 Additionally, three groups of three animals were inoculated with either 10<sup>4</sup>, 10<sup>5</sup> or 10<sup>6</sup> TCID<sub>50</sub>  
68 SARS-CoV-2 and swabs were taken for four days before the animals were euthanized and  
69 autopsied. All animals inoculated with 10<sup>6</sup> TCID<sub>50</sub> were viral RNA positive in the nose and  
70 throat for at least four days with a single animal positive in the rectum at day three (Figure 2,  
71 panel C). Animals inoculated with 10<sup>5</sup> TCID<sub>50</sub> were RNA positive in the nose for at least four  
72 days, for at least three days in the throat but not in the rectum (Figure 2, panel D). These animals  
73 also shed infectious virus in the nose for up to three days (mean shedding of 1.67 days, SD=1.53)  
74 and one animal shed virus two days post infection in the throat (data not shown). Animals  
75 inoculated with 10<sup>4</sup> TCID<sub>50</sub> did not shed any detectable viral RNA (Figure 2, panel E). Although  
76 nasal turbinates yielded on average 8.42x10<sup>3</sup> RNA copies/ml, lung homogenates of animals  
77 inoculated with 10<sup>6</sup> TCID<sub>50</sub> virus were found viral RNA negative (Figure 2, panel F). Despite the  
78 fact that no viral RNA was detected in the lungs, histological examination of the lungs of  
79 infected animals sacrificed four days p.i. revealed a multifocal mild to moderate increase in  
80 alveolar macrophages in the alveolar lumina with multifocal presence of few neutrophils. Mainly  
81 associated with the terminal bronchioles, multifocal mild thickening of the septa, with  
82 infiltrations of neutrophils, eosinophils and occasional lymphocytes, plasma cells and  
83 macrophages was observed (Figure 2, panel G). Mild multifocal necrosis of alveolar epithelial  
84 cells and the presence of a few enlarged, syncytial cells in the alveolar lumina were seen (Figure  
85 2, panel H). There was mild peribronchiolar and peribronchial lymphoplasmacytic infiltration  
86 with eosinophils and moderate to severe bronchus-associated lymphoid tissue proliferation

87 (Supplementary figure 1, panel A). Some animals showed enlarged tracheo-bronchial lymph  
88 nodes consistent with mild lymphoid hyperplasia. In the nose, there was multifocal infiltration of  
89 moderate numbers of eosinophils and lymphoplasmacytic infiltrates in the olfactory epithelium  
90 (exocytosis) and in the lamina propria, alongside mild hyperplasia and hypertrophy of the  
91 olfactory epithelium (Supplementary figure 1, panel B). Mild eosinophilic exocytosis was  
92 present in the trachea.

### 93 **Conclusions**

94 This study demonstrates that rabbits are susceptible to SARS-CoV-2. While the infection  
95 is asymptomatic, infectious virus with peak titers corresponding to  $\sim 10^3$  TCID<sub>50</sub> could be  
96 detected up to day seven post inoculation in the nose. The minimum dose to establish productive  
97 infection was  $10^5$  TCID<sub>50</sub>, indicating that virus transmission between rabbits may be less  
98 efficient compared to ferrets and hamsters. The use of young, immunocompetent, and healthy  
99 New Zealand White rabbits in this study however may not reflect virus shedding and disease in  
100 other rabbit breeds or rabbits at different ages. Thus, surveillance studies - including serological  
101 testing - may be needed to assess the presence of SARS-CoV-2 in farmed rabbits.

102 Viral shedding in rabbits occurred in a biphasic pattern, which was also observed for  
103 SARS-CoV-2 infected African green monkeys (10). This pattern is potentially linked to early  
104 innate immune responses that act within days, followed by adaptive responses that generally take  
105 one week to be activated. These observations are in line with recent findings that the presence of  
106 neutralizing serum antibodies in humans negatively correlates with infectious virus shedding,  
107 and that shedding of viral RNA outlasts shedding of infectious virus (11). The presence of  
108 eosinophils in the nose and lungs of infected animals suggests a possible helper T cell 2 (Th2)-  
109 mediated immune response. The preferential upper respiratory tract infection in the absence of

110 robust replication in the lower respiratory tract of rabbits resembles what has been observed in  
111 experimentally inoculated ferrets (5).

112 The transmission of SARS-CoV-2 to mink caused viral spread between farm animals  
113 and spillover to humans, resulting in mass culling of mink to limit the spread of the virus (6).  
114 This study provides evidence of susceptibility of rabbits to SARS-CoV-2 infection warranting  
115 further investigations on the presence of SARS-CoV-2 in farmed rabbits.

116

## 117 **Acknowledgments**

118 This research is partly financed by the Netherlands Organization for Health Research and  
119 Development (ZONMW) grant agreement 10150062010008 to B.L.H and co-funded by the PPP  
120 Allowance (grant agreement LSHM19136) made available by Health Holland, Top Sector Life  
121 Sciences & Health, to stimulate public-private partnerships.

122

## 123 **Author Bio**

124 Anna Mykytyn is a PhD candidate at Erasmus Medical Centre, Rotterdam. Her research interests  
125 are the pathogenesis and transmission of coronaviruses including SARS-CoV-2.

126

127

128

129

130 **References**

- 131 1. World Health Organization. Coronavirus disease (COVID-19) pandemic. 2020 [cited;  
132 Available from: <https://www.who.int/emergencies/diseases/novel-coronavirus-2019>
- 133 2. Chan JF, Zhang AJ, Yuan S, Poon VK, Chan CC, Lee AC, et al. Simulation of the  
134 clinical and pathological manifestations of Coronavirus Disease 2019 (COVID-19) in golden  
135 Syrian hamster model: implications for disease pathogenesis and transmissibility. *Clin Infect*  
136 *Dis*. 2020 Mar 26.
- 137 3. Rockx B, Kuiken T, Herfst S, Bestebroer T, Lamers MM, Oude Munnink BB, et al.  
138 Comparative pathogenesis of COVID-19, MERS, and SARS in a nonhuman primate model.  
139 *Science*. 2020 May 29;368(6494):1012-5.
- 140 4. Sia SF, Yan LM, Chin AWH, Fung K, Choy KT, Wong AYL, et al. Pathogenesis and  
141 transmission of SARS-CoV-2 in golden hamsters. *Nature*. 2020 May 14.
- 142 5. Shi J, Wen Z, Zhong G, Yang H, Wang C, Huang B, et al. Susceptibility of ferrets, cats,  
143 dogs, and other domesticated animals to SARS–coronavirus 2. *Science*. 2020:eabb7015.
- 144 6. Oreshkova N, Molenaar R-J, Vreman S, Harders F, Munnink BBO, Hakze R, et al.  
145 SARS-CoV2 infection in farmed mink, Netherlands, April 2020. *bioRxiv*.  
146 2020:2020.05.18.101493.
- 147 7. Zhou P, Yang XL, Wang XG, Hu B, Zhang L, Zhang W, et al. A pneumonia outbreak  
148 associated with a new coronavirus of probable bat origin. *Nature*. 2020 Mar;579(7798):270-3.
- 149 8. Li F. Structure, Function, and Evolution of Coronavirus Spike Proteins. *Annu Rev Virol*.  
150 2016 Sep 29;3(1):237-61.
- 151 9. Zhao X, Chen D, Szabla R, Zheng M, Li G, Du P, et al. Broad and differential animal  
152 ACE2 receptor usage by SARS-CoV-2. *J Virol*. 2020 Jul 13.

- 153 10. Hartman AL, Nambulli S, McMillen CM, White AG, Tilston-Lunel NL, Albe JR, et al.  
154 SARS-CoV-2 infection of African green monkeys results in mild respiratory disease discernible  
155 by PET/CT imaging and prolonged shedding of infectious virus from both respiratory and  
156 gastrointestinal tracts. bioRxiv. 2020:2020.06.20.137687.
- 157 11. van Kampen JJA, van de Vijver DAMC, Fraaij PLA, Haagmans BL, Lamers MM, Okba  
158 N, et al. Shedding of infectious virus in hospitalized patients with coronavirus disease-2019  
159 (COVID-19): duration and key determinants. medRxiv. 2020:2020.06.08.20125310.

160

161

162

163

164

165

166

167

168

169

170

171

172

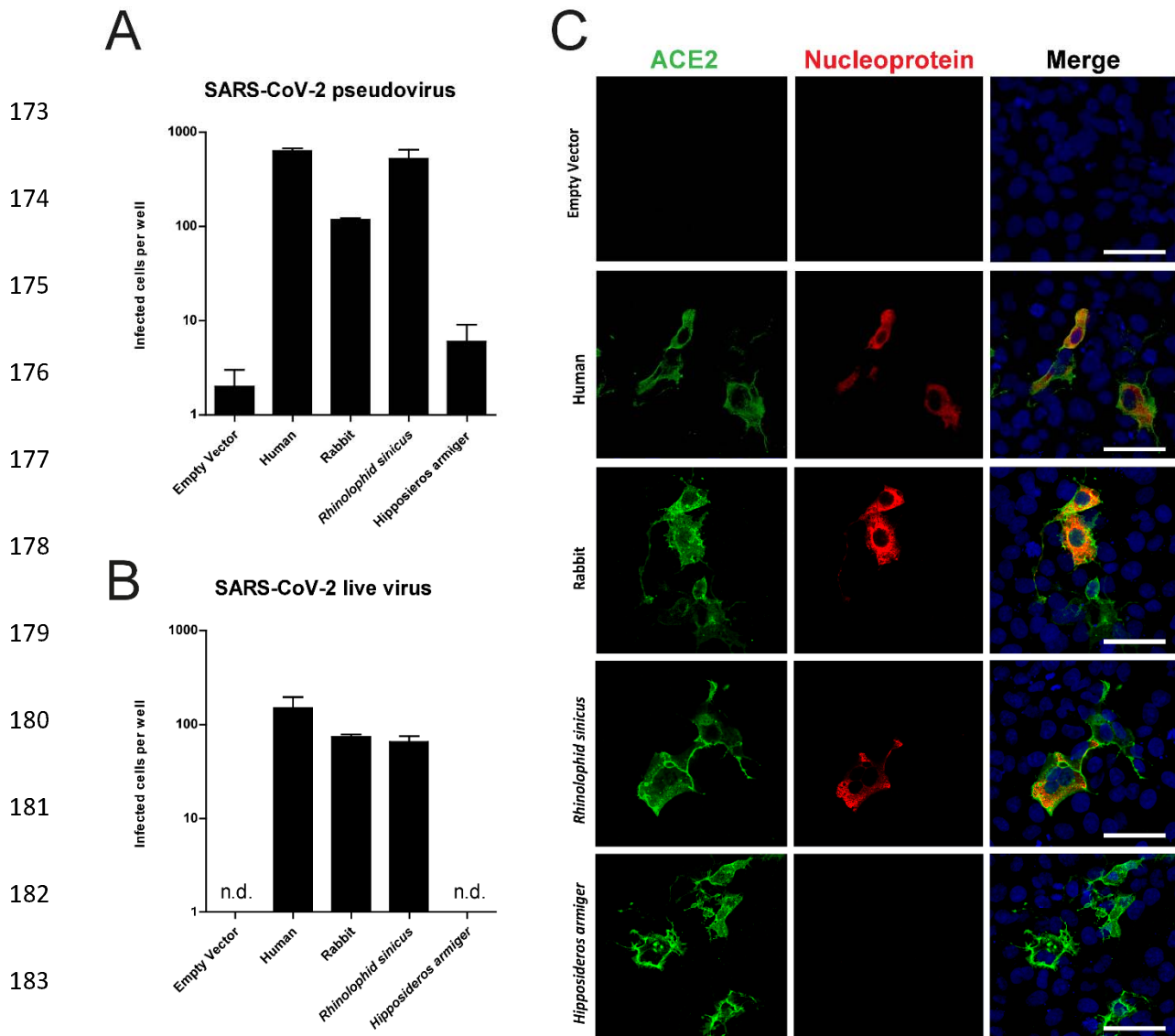


**Figure 1. Rabbit ACE2 mediated SARS-CoV-2 infection.** SARS-CoV-2 pseudovirus (A) and authentic virus (B) infection of Cos-7 cells expressing ACE2 of various species. Infectivity was quantified by staining live virus cells with anti-SARS-CoV nucleocapsid and scanning live virus and pseudovirus infected cells. (C) Confocal imaging of ACE2 mediated live virus infection; cells were stained using anti-human ACE2 in green, anti-SARS-CoV nucleocapsid in red and TO-PRO3 in blue to stain nuclei. Scale indicates 50 $\mu$ m.

187

188

189

190

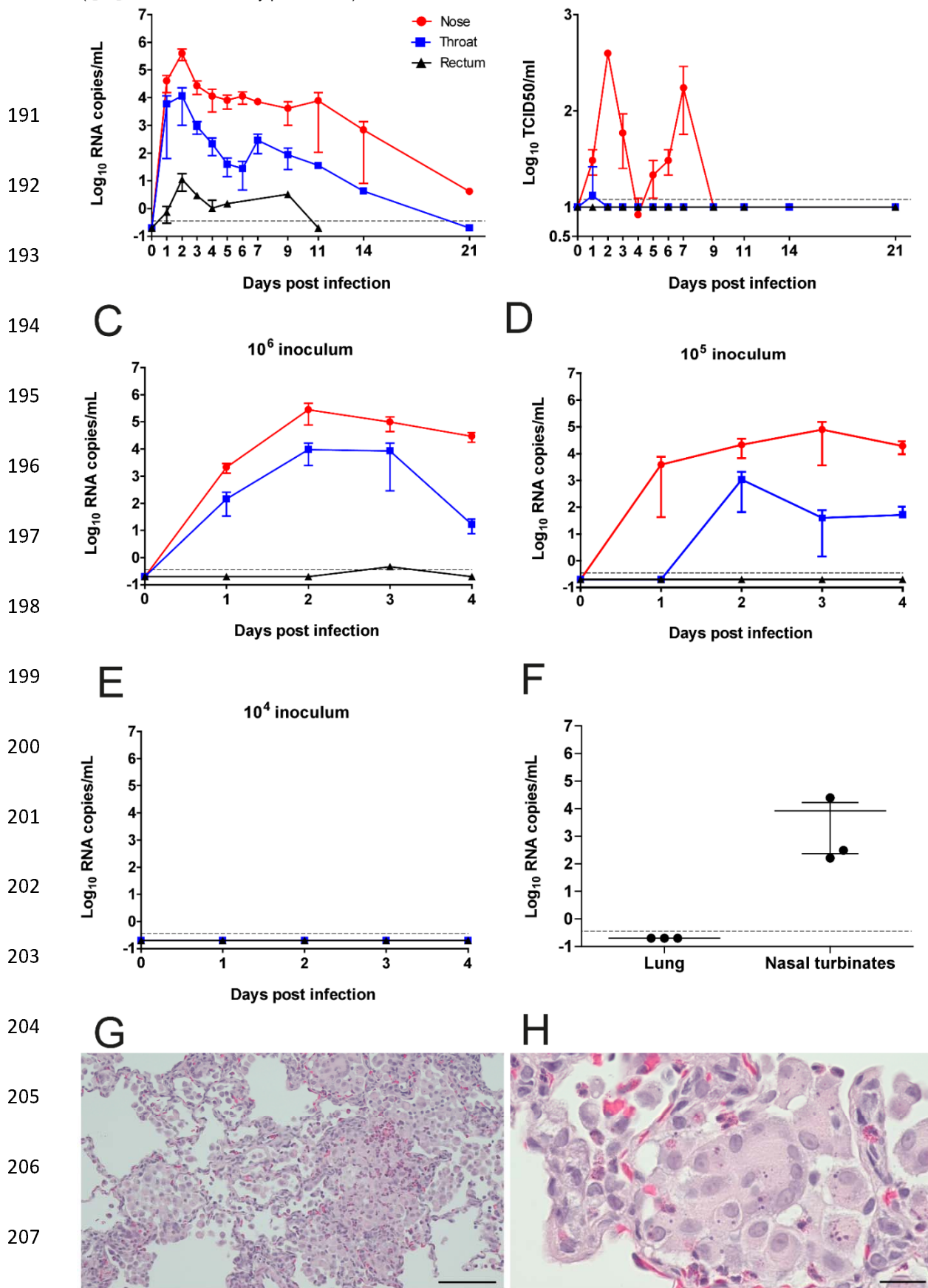


**Figure 2. Susceptibility of rabbits to SARS-CoV-2 infection.** Infection kinetics of (A) viral RNA and (B) authentic SARS-CoV-2 virus growth curves from rabbits inoculated with  $10^6$  TCID<sub>50</sub> and followed up for 21 days. (C-E) Viral RNA growth curves in rabbits inoculated with either (C)  $10^6$ , (D)  $10^5$ , or (E)  $10^4$  TCID<sub>50</sub> and followed up for four days post infection. (F) Viral RNA in lung and nasal turbinates of  $10^6$  TCID<sub>50</sub> infected rabbits, sacrificed after four days. RNA detection limits were set at  $3.5 \times 10^{-1}$  RNA copies/ml, while live virus detection limit was 12 TCID<sub>50</sub>/ml. (G, H) Histopathological analysis of lungs from rabbits inoculated with  $10^6$  TCID<sub>50</sub>, sacrificed after four days. (G) Alveolar thickening and inflammatory infiltrates. Scale indicates 100µm (H) Enlarged,

209 **Supplementary**

210 **Materials and Methods**

211 **Expression plasmids and cloning**

212 Plasmids in pcDNA3.1 encoding human ACE2 (OHu20260), rabbit ACE2 (Clone ID  
213 OOb21562D), *Rhinolophus sinicus* ACE2 (ORh96277) and *Hipposideros armiger* ACE2 (Clone  
214 ID OHi02685) were ordered from GenScript. Codon-optimized cDNA encoding SARS-CoV-2 S  
215 glycoprotein (isolate Wuhan-Hu-1) with a C-terminal 19 amino acid deletion was synthesized  
216 and cloned into pCAGSS in between the EcoRI and BglII sites. pVSV-eGFP-dG (#31842),  
217 pMD2.G (#12259), pCAG-VSV-P (#64088), pCAG-VSV-L (#64085), pCAG-VSV-N (#64087)  
218 and pCAGGS-T7Opt (#65974) were ordered from Addgene. S expressing pCAGGS vectors  
219 were used for the production of pseudoviruses, as described below.

220 **Cell lines**

221 HEK-293T cells were maintained in Dulbecco's Modified Eagle's Medium (DMEM, Gibco)  
222 supplemented with 10% fetal bovine serum (FBS), 1X non-essential amino acids (Lonza), 1mM  
223 sodium pyruvate (Gibco), 2mM L-glutamine (Lonza), 100 µg/ml streptomycin (Lonza) and 100  
224 U/ml penicillin. Cos-7, Vero, and VeroE6 cells were maintained in DMEM supplemented with  
225 10% FBS, 1.5 mg/ml sodium bicarbonate (Lonza), 10mM HEPES (Lonza), 2mM L-  
226 glutamine, 100 µg/ml streptomycin and 100 U/ml penicillin. All cell lines were maintained at  
227 37°C in a 5% CO<sub>2</sub> humidified incubator.

228 **VSV delta G rescue**

229 The protocol for VSV-G pseudovirus rescue was adapted from Whelan and colleagues (1).  
230 Briefly, a 70% confluent 10 cm dish of HEK-293T cells was transfected with 10µg pVSV-eGFP-  
231 ΔG, 2µg pCAG-VSV-N (nucleocapsid), 2µg pCAG-VSV-L (polymerase), 2µg pMD2.G  
232 (glycoprotein, VSV-G), 2µg pCAG-VSV-P (phosphoprotein) and 2µg pCAGGS-T7Opt (T7  
233 RNA polymerase) using polyethylenimine (PEI) at a ratio of 1:3 (DNA:PEI) in Opti-MEM I  
234 (1X) + GlutaMAX. Forty-eight hours post-transfection the supernatant was transferred onto new  
235 plates transfected 24 hours prior with VSV-G. After a further 48 hours, these plates were re-  
236 transfected with VSV-G. After 24 hours the resulting pseudoviruses were collected, cleared by  
237 centrifugation at 2000 x g for 5 minutes, and stored at -80°C. Subsequently, VSV-G pseudovirus  
238 batches were produced by infecting VSV-G transfected HEK-293T cells with VSV-G  
239 pseudovirus at a MOI of 0.1. Titres were determined by preparing 10-fold serial dilutions in  
240 Opti-MEM I (1X) + GlutaMAX. Aliquots of each dilution were added to monolayers of 2 ×  
241 10<sup>4</sup> Vero cells in the same medium in a 96-well plate. Three replicates were performed per  
242 pseudovirus stock. Plates were incubated at 37°C overnight and then scanned using an  
243 Amersham Typhoon scanner (GE Healthcare). Individual infected cells were quantified using  
244 ImageQuant TL software (GE Healthcare). All pseudovirus work was performed in a Class II  
245 Biosafety Cabinet under BSL-2 conditions at Erasmus Medical Center.

#### 246 **Coronavirus S pseudovirus production**

247 For the production of SARS-CoV-2 S pseudovirus, HEK-293T cells were transfected with 10 µg  
248 S expression plasmids. Twenty-four hours post-transfection, the medium was replaced for Opti-  
249 MEM I (1X) + GlutaMAX, and cells were infected at an MOI of 1 with VSV-G pseudovirus.  
250 Two hours post-infection, cells were washed three times with OptiMEM and replaced with  
251 medium containing anti-VSV-G neutralizing antibody (clone 8G5F11; Absolute Antibody) at a

252 dilution of 1:50,000 to block remaining VSV-G pseudovirus. The supernatant was collected after  
253 24 hours, cleared by centrifugation at 2000 x g for 5 minutes and stored at 4°C until use within 7  
254 days. SARS-CoV-2 pseudovirus was titrated on VeroE6 cells as described above.

#### 255 **Virus stock**

256 SARS-CoV-2 (isolate BetaCoV/Munich/BavPat1/2020; European Virus Archive Global #026V-  
257 03883; kindly provided by Dr. C. Drosten) was propagated on Vero E6 (ATCC® CRL 1586™)  
258 cells in OptiMEM I (1X) + GlutaMAX (Gibco), supplemented with penicillin (100 IU/mL) and  
259 streptomycin (100 IU/mL) at 37°C in a humidified CO<sub>2</sub> incubator. Stocks were produced by  
260 infecting Vero E6 cells at a multiplicity of infection (MOI) of 0.01 and incubating the cells for  
261 72 hours. The culture supernatant was cleared by centrifugation and stored in aliquots at -80°C.  
262 Stock titers were determined by titration on VeroE6 cells. The TCID<sub>50</sub> was calculated according to  
263 the method of Spearman & Kärber (ref?). All work with infectious SARS-CoV-2 was performed  
264 in a Class II Biosafety Cabinet under BSL-3 conditions at Erasmus Medical Center.

#### 265 **Pseudovirus and live virus infection *in vitro***

266 Cos-7 cells plated at 70% density in a 24 well format were transfected 24 hours after plating by  
267 dropwise addition of 500 ng ACE2 expression plasmids using a PEI ratio of 1:3 (DNA:PEI) in  
268 Opti-MEM I (1X) + GlutaMAX. After 24 hours, cells were washed twice and replaced with fresh  
269 Opti-MEM I (1X) + GlutaMAX prior to pseudovirus or live virus infection. Pseudovirus  
270 transduction was performed by infecting plates with 10<sup>3</sup> VeroE6 titrated particles per well. Plates  
271 were incubated for 16 hours at 37°C before quantifying GFP-positive cells using an Amersham  
272 Typhoon scanner and ImageQuant TL software. Authentic virus infection was performed by  
273 adding 10<sup>4</sup> TCID<sub>50</sub> SARS-CoV-2 per well and incubating plates for 8 hours at 37°C. After

274 incubation, cells were formalin fixed, permeabilized with 70% ethanol and stained with 1:1000  
275 mouse anti-SARS nucleoprotein (Sino Biological) and 1:1000 rabbit anti-human ACE2  
276 (Abcam), followed by 1:1000 goat anti-rabbit Alexa-Fluor 594, 1:1000 goat anti-mouse Alexa-  
277 Fluor 488, and 1:1000 TO-PRO3 (Thermo Fisher) to stain nuclei. Quantification of virus  
278 infected cells was performed using an Amersham Typhoon scanner and ImageQuant TL software  
279 as described above, while confocal imaging was performed on a LSM700 confocal microscope  
280 using ZEN software (Zeiss).

### 281 ***In vivo* study design**

282 Animal experiments were approved and performed according to the guidelines from the  
283 Institutional Animal Welfare Committee (AVD277002015283-WP04). The studies were  
284 performed under biosafety level 3 (BSL3) conditions. Three month-old New Zealand White  
285 rabbits (*Oryctolagus cuniculus*), specific pathogen free, and seronegative for SARS-CoV-2 were  
286 divided into four groups of three animals. Animals were inoculated under ketamine-  
287 medetomidine anesthesia intranasally with 1 ml SARS-CoV-2 (0.5 ml per nostril). Three groups  
288 were infected intranasally with respectively  $10^4$ ,  $10^5$  or  $10^6$  TCID<sub>50</sub> SARS-CoV-2 and monitored  
289 for four days post infection, and an additional three animals were infected with  $10^6$  TCID<sub>50</sub>  
290 SARS-CoV-2 and monitored for 21 days post infection. Animals monitored for four days were  
291 swabbed from the nose, throat, and rectum daily before being sacrificed for pathology on day 4  
292 post infection. The remaining three  $10^6$  TCID<sub>50</sub> infected animals were followed until 21 days  
293 post infection with swabs taken on days zero to seven, then on days nine, 11, 14 and 21 post  
294 infection. In addition, on day 21 sera was collected from these animals for serological testing.

295 **Plaque reduction neutralization test 50 (PRNT<sub>50</sub>)**. Serum samples were tested for their  
296 neutralization capacity against SARS-CoV-2 as described before (2). Heat-inactivated (56

297 degrees Celsius for 30 minutes) samples were 2-fold serially diluted in Dulbecco modified Eagle  
298 medium supplemented with NaHCO<sub>3</sub>, HEPES buffer, penicillin, streptomycin, and 1% fetal  
299 bovine serum, starting at a dilution of 1:10 in 50 µL. Fifty µL virus suspension (~400 plaque-  
300 forming units) was added to each well and incubated at 37°C for 1 hour before transferring to  
301 VeroE6 cells. After incubation cells were washed and supplemented with medium, followed by  
302 an 8 hour incubation. After incubation, the cells were fixed with 4% formaldehyde/phosphate-  
303 buffered saline (PBS) and stained with polyclonal rabbit anti-SARS-CoV antibody (Sino  
304 Biological), followed by a secondary peroxidase-labeled goat anti-rabbit IgG (Dako). The signal  
305 was developed by using a precipitate forming 3,3',5,5' tetramethylbenzidine substrate (True  
306 Blue; Kirkegaard and Perry Laboratories) and the number of infected cells per well was  
307 quantified using an ImmunoSpot Image Analyzer (CTL Europe GmbH). The serum  
308 neutralization titer is the reciprocal of the highest dilution resulting in an infection reduction of  
309 >50% (PRNT<sub>50</sub>). A titer >20 was considered positive.

### 310 **RNA extraction and qRT-PCR**

311 Swabs, lung homogenates and nasal turbinate homogenates were thawed and centrifuged at  
312 2,000 x g for 5 min. Sixty µL supernatant was lysed in 90 µL MagnaPure LC Lysis buffer  
313 (Roche) at room temperature for 10 minutes. RNA was extracted by incubating samples with 50  
314 µL Agencourt AMPure XP beads (Beckman Coulter) for 15 minutes at room temperature,  
315 washing beads twice with 70% ethanol on a DynaMag-96 magnet (Invitrogen) and eluting in 30  
316 µL ultrapure water. RNA copies per mL were determined by qRT-PCR using primers targeting  
317 the E gene (37) and compared to a counted RNA standard curve.

### 318 **Histopathology**

319 Alveolitis severity, bronchitis/bronchiolitis severity, tracheitis and rhinitis severity were scored:  
320 0 = no inflammatory cells, 1 = few inflammatory cells, 2 = moderate number of inflammatory  
321 cells, 3 = many inflammatory cells. Alveolitis extent, 0 = 0%, 1 = <25%, 2 = 25-50%, 3 = >50%.  
322 Alveolar oedema presence, alveolar haemorrhage presence, type II pneumocyte hyperplasia  
323 presence, 0 = no, 1 = yes. Extent of peribronchial/perivascular cuffing, 0 = none, 1 = 1-2 cells  
324 thick, 2 = 3-10 cells thick, 3 = >10 cells thick.

### 325 **Immunohistochemistry**

326 Semiquantitative assessment of SARS-CoV-2 viral antigen expression in the lungs was  
327 performed as reported for SARS-CoV earlier (3) with a few amendments: for the alveoli, twenty-  
328 five arbitrarily chosen, 20x objective fields of lung parenchyma in each lung section were  
329 examined by light microscopy for the presence of SARS-CoV-2 nucleoprotein, without the  
330 knowledge of the allocation of the animals. The cumulative scores for each animal were  
331 presented as number of positive fields per 100 fields. For the bronchi and bronchioles, the  
332 percentage of positively staining bronchial and bronchiolar epithelium was estimated on every  
333 slide and the average of the four slides was taken to provide the score per animal. For the trachea  
334 and nose, the percentage of positively staining epithelium was estimated on every slide.

### 335 **References**

336 1. Whelan SP, Ball LA, Barr JN, Wertz GT. Efficient recovery of infectious vesicular  
337 stomatitis virus entirely from cDNA clones. Proc Natl Acad Sci U S A. 1995 Aug  
338 29;92(18):8388-92.

339 2. Okba NMA, Muller MA, Li W, Wang C, GeurtsvanKessel CH, Corman VM, et al.  
340 Severe Acute Respiratory Syndrome Coronavirus 2-Specific Antibody Responses in Coronavirus  
341 Disease Patients. *Emerg Infect Dis.* 2020 Jul;26(7):1478-88.

342 3. Haagmans BL, Kuiken T, Martina BE, Fouchier RA, Rimmelzwaan GF, van Amerongen  
343 G, et al. Pegylated interferon-alpha protects type 1 pneumocytes against SARS coronavirus  
344 infection in macaques. *Nat Med.* 2004 Mar;10(3):290-3.

345

### 346 **Supplementary Figures**

347

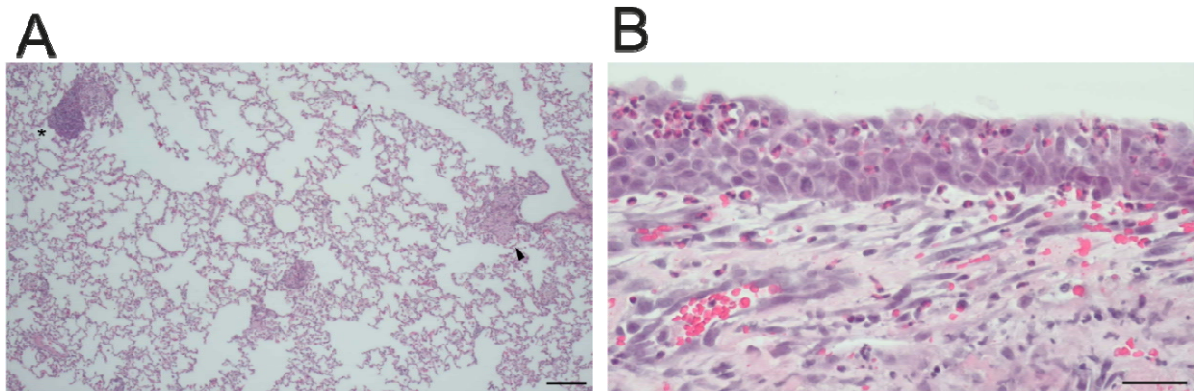
348

349

350

351

352



353 **Supplementary Figure 1. Lung histology of SARS-CoV-2 infected rabbits.** (A) Lung  
354 pathology overview from rabbits inoculated with  $10^6$  TCID<sub>50</sub> and sacrificed 4 days post infection.  
355 Arrow indicates thickening and asterisk bronchus-associated lymphoid tissue (BALT). Scale  
356 indicates 200 $\mu$ m. (B) Eosinophilic infiltrates in the nose. Scale indicates 40 $\mu$ m.

355

356

357